# Quantum size effects in nanostructures

**Lecture notes to the course**
***Organic and Inorganic Nanostructures***

***Kjeld Pedersen***

**Department of Physics and Nanotechnology**
**Aalborg University**

Aalborg, August 2006

## 1. Introduction

One of the most direct effects of reducing the size of materials to the nanometer range is the appearance of quantization effects due to the confinement of the movement of electrons. This leads to discrete energy levels depending on the size of the structure as it is known from the simple potential well treated in introductory quantum mechanics. Following this line artificial structures with properties different from those of the corresponding bulk materials can be created. Control over dimensions as well as composition of structures thus makes it possible to tailor material properties to specific applications.
Both semiconductor and metal nanostructures have been investigated over the years. While the applications of metal nanostructures are still very limited semiconductor electronic and optoelectronic components based on structures with quantum size effects have been on the market for several years. The present notes will therefore treat the size effects with semiconductor materials like GaAs in mind.
It is very rare that the nanostructures appear as free standing structures. Rather, they are embedded in a matrix material that necessarily has an effect on the electronic levels in the nanostructure. In the rather simple treatments presented here it is not possible to take the matrix materials into account. However, the simple models still give good impressions of the basic principles behind quantum size effects in various structures.
The nanostructures treated here can be divided into the following classes:
**Two-dimensional objects:** Thin films with thickness of the order of a few nanometers are usually deposited on a bulk material. Their properties may be dominated by surface and interface effects or they may reflect the confinement of electrons in the direction perpendicular to the film (a quantum well). In the two dimensions parallel to the film the electrons behave like in a bulk material.
**One-dimensional objects:** Cylinder-like objects like wires and tubes with diameters on the nanoscale and lengths typically in the micometer range. Also embedded structures with rectangular cross section exist. Confinement effects for electrons may appear in the transverse direction while electrons are free to move in one dimension (along the structure).
**Zero- dimensional objects**: Usual names are nanoparticles, clusters, colloids, nanocrystals, and fullerenes. They are composed of several tens to a few thousand atoms. Electrons are confined in all three directions.
**Carbon nanotubes:** They can be described as graphene sheets rolled into cylinders. Single walled tubes have diameters of the order of 1-2 nm. The confinement effects can here be seen as the adjustment of electronic wavefunctions to fit to the circumfence of the tube.

It should be noted that many applications of nanostructures do not depend directly on size effects on electronic properties. Instead, the surface to volume ratio may lead to mew functionalities, for instance in catalytic effects. Intensive research is directed toward introduction of new functionalitites to matrix materials without affecting other material properties by introduction of nanosized structures.

At the end of these notes some useful references with more detailed treatments of nanostructures and their optical properties are given.

## 2. Quantum wells, wires, and dots

In this section we will go through a sequence of structures with increasing confinement of electrons from the potential barriers at the boundaries of the structures.

### 2.1 Two-dimensional objects

In this type of systems the electron are confined in their motion in one direction while they move as in the corresponding bulk material in the other two directions. Today these effects are widely used in semiconductor lasers where the band structure of quantum wells are tailored to give the desired emission wavelengths. The classic example of a semiconductor quantum well is the GaAs – $Al_xGa_{(1-x)}As$ multilayer system. Here the depth of the well can be adjusted through the composition of th e AlGaAs layer (Fig. 2.1). Generally, we distinguish between quantum well structures and superlattices. The two structures are illustrated in Fig. 2.2. If the distance between the potential wells is so large that the wave functions of the bound states have little overlap we talk about quantum wells. If, on the other hand the wave functions overlap the structure is usually called a superlattice.

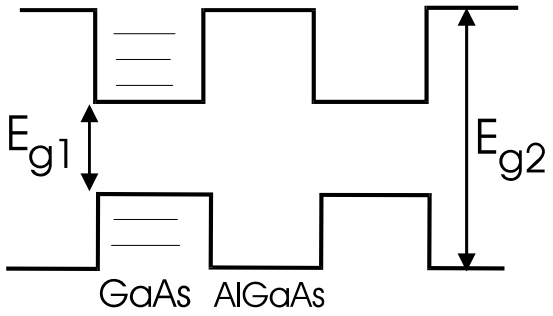


Fig. 2.1 Quantum well structure formed in GaAs layers sandwiched between AlGaAs layers.

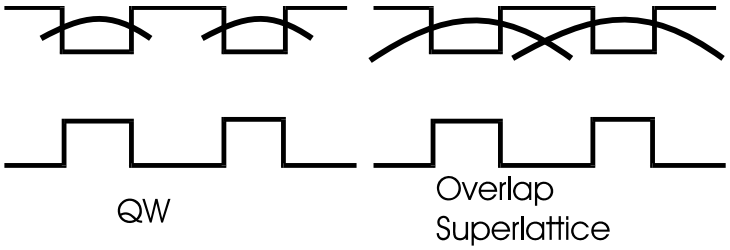


Fig. 2.2. Quantum well and super lattice structures.

In the following we will consider a single quantum well as illustrated on Fig. 2.3. In order to describe wave functions and energy levels we start with the Schrödinger equation:

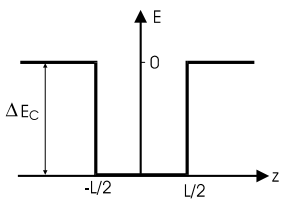


Fig. 2.3. A simple potential well.

$$\left[-\frac{\hbar^2}{2m_{\|}}\frac{\partial^2}{\partial r_{\|}^{\,2}}-\frac{\hbar^2}{2m_z}\frac{\partial^2}{\partial z^2}+V(z)\right]\phi(\vec{r})=E\phi(\vec{r})\,. \qquad (2.1)$$

This is a second-order differential equation in space coordinates. We will treat the parallel and z- directions as independent and thus separate the variables according to:

$$\phi(\vec{r})=\phi_{\|}(\vec{r}_{\|})\phi_n(z)\,. \qquad (2.2)$$

We will then have two independent differential equations:

$$\left[-\frac{\hbar^2}{2m_z}\frac{\partial^2}{\partial z^2}+V(z)\right]\phi_n(z)=E_n\phi(z) \tag{2.3}$$

$$-\frac{\hbar^2}{2m_{\|}}\frac{\partial^2}{\partial r_{\|}^{\,2}}\phi_{\|}(\vec{r}_{\|})=(E-E_n)\phi_{\|}(\vec{r}_{\|})\,. \tag{2.4}$$

Let us start by considering z-dependent part which includes the size-dependence in the electronic levels. At first let us look at the solution for infinite barriers, that is $\Delta E_C \to \infty$. The wave functions must then be zero at the borders of the well (and outside the well): $\phi_n(L/2)=\phi_n(-L/2)=0$. These boundary conditions are fulfilled by wave functions of the form

$$\phi_n=\begin{cases}\sqrt{2/L}\cos\left(\dfrac{n\pi z}{L}\right) & n=1,3,5,\cdots \ even\\[2ex] \sqrt{2/L}\sin\left(\dfrac{n\pi z}{L}\right) & n=2,4,6,\cdots \ odd\,.\end{cases} \tag{2.5}$$

For growing *n* the wave functions are alternatively even and odd functions of z (Fig. 2.4). The corresponding energies are given by

$$E_n=\frac{\hbar^2}{2m_z}\left(\frac{n\pi}{L}\right)^2 \quad for\ n=1,2,3,\cdots. \tag{2.6}$$

This gives a first impression of the symmetries of wave functions and the order of magnitude of the discrete energy levels appearing as a result of the finite thickness of the well. Notice that separation between energy levels decrease as the thickness of the well increases. The infinite well approximation is however usually far from useful predictions in real systems. We thus have to deal with finite barrier wells.

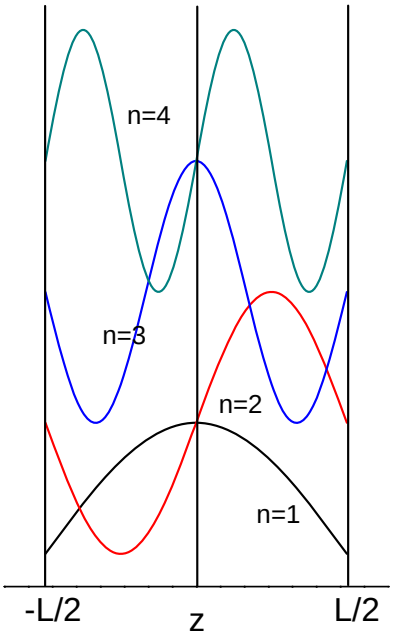


In the following we will consider bound states, that is $E<\Delta E_C$. Outside the well we expect exponentially decaying wave functions while *cos* and *sin* functions still work inside the well. The form of $\phi_n(z)$ will then be

$$\phi_n=\begin{cases}A\cos(kz) & |z|<L/2 \quad even\\ A\sin(kz) & |z|<L/2 \quad odd\\ B\exp\left[-\alpha\left(z-L/2\right)\right] & z>l/2\\ B\exp\left[\alpha\left(z-L/2\right)\right] & z<-l/2\,.\end{cases} \tag{2.7}$$

Fig. 2.4. Alternating odd and even wavefunctions in an infinitely deep well.

The energies are given by

$$E_n = \begin{cases} \dfrac{\hbar^2 k^2}{2m_A} - \Delta E_C & \textit{inside the well} \\ -\dfrac{\hbar^2 \alpha^2}{2m_B} & \textit{outside the well.} \end{cases} \tag{2.8}$$

Indices A and B indicate that the effective masses usually differ in the two materials forming the well and its surroundings. Zero energy is taken at the top of the well. Electrons with negative energy are thus confined to the well while those with positive energy are free to move through the structure.

To determine the constants A and B as well as the wave vector *k* and damping rate $\alpha$ we introduce boundary conditions for the wave function at the interface ($z = \pm L/2$) between the two materials:

$$\begin{aligned} &\phi_n \quad \textit{continous} \\ &\frac{1}{m_z}\frac{d\phi_n}{dz} \quad \textit{continous} \end{aligned} \tag{2.9}$$

The last equation states that the particle current is continuous. For the even part these two conditions lead to

$$\begin{aligned} &B = \cos\left(\frac{kL}{2}\right) \quad \textit{from } \phi_n \textit{ continuous} \\ &\frac{kA}{m_A}\sin\left(\frac{kL}{2}\right) = \frac{\alpha B}{m_B} \quad \textit{from } \frac{d\phi_n}{dz} \textit{ continuous}. \end{aligned} \tag{2.10}$$

In order to find solutions for k and α we take the ratio between these two equations and also between the corresponding two equations for the odd wave function, which leads to

$$\begin{aligned} &\frac{k}{m_A}\tan\left(\frac{kL}{2}\right) = \frac{\alpha}{m_B} \\ &\frac{k}{m_A}\cot\left(\frac{kL}{2}\right) = -\frac{\alpha}{m_B}. \end{aligned} \tag{2.11}$$

These two equations can not be solved analytically. They are however quite simple to solve numerically. To illustrate the solutions graphically let us rewrite the equations by expressing α from the energy equation and assume $m_A = m_B$

$$\alpha^2 = \frac{2m\Delta E_C}{\hbar^2} - k^2. \tag{2.12}$$

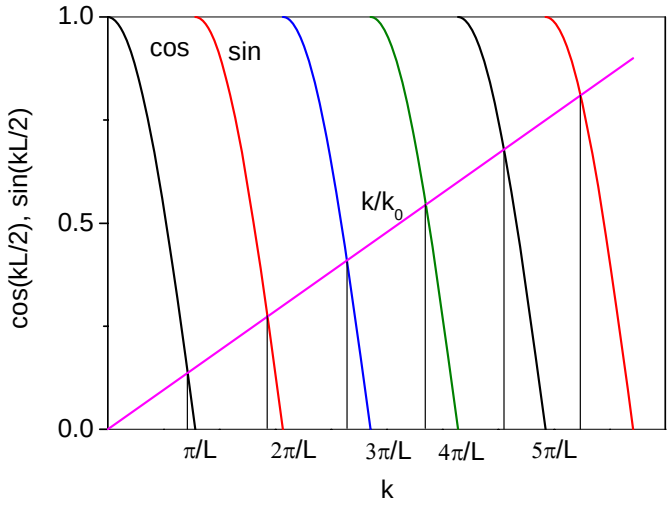


Fig. 2.5. Graphical solutions to Eqs. (2.13).

Inserting this in the two transcendent equations above leads to

$$\cos\left(\frac{kL}{2}\right)=\frac{k}{k_0} \qquad \sin\left(\frac{kL}{2}\right)=\frac{k}{k_0} \tag{2.13}$$

with $k_0^2=\frac{2m\Delta E_C}{\hbar^2}$ as the maximum value of $k$.

Figure 2.5 shows plots of right and left hand sides of Eqs. (2.13). Solutions giving the discrete allowed values of $k$ are marked with vertical lines. With the values of $k$ known the discrete energy levels can be calculated.

Exercise: What determines the number of discrete levels in a well?

Having solved the z-dependent part of the Schrödinger equation we will turn to the parallel part. Generally the solution will have the 2D Bloch form

$$\phi\left(\vec{r}_{\|}\right)=\sum_{A,B}U_k^{A,B}\left(\vec{r}_{\|}\right)e^{i\vec{k}_{\|}\cdot\vec{r}} \tag{2.14}$$

where $U_k$ is periodic in the lattice of respectively material A and B. In the free electron case simple parabolic bands are obtained and the total energy of the electrons is given by

$$E\left(k_{\|},n\right)=E_n+\frac{\hbar^2k_{\|}^2}{2m_{\|}}. \tag{2.15}$$

The discrete energies $E_n$ will thus increase quadratically with the parallel wave vector $k_{||}$.

## 2.2. Density of states for free electrons

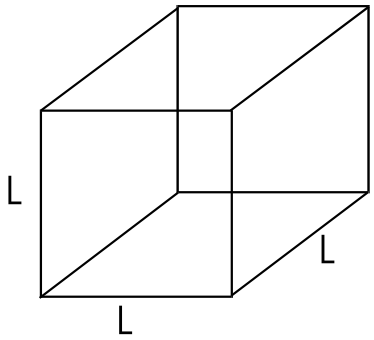


Fig. 2.6.

The density of states is a very useful quantity when we want to look at optical spectra. Let us assume the electrons are confined to a box of dimensions L in all three directions (Fig. 2.6). The solution to the free electron Schrödinger equation is in the form of plane waves

$$\psi\left(\vec{r}\right)=e^{i\vec{k}\cdot\vec{r}}. \tag{2.16}$$

Introducing periodic boundary conditions of the form

$$\psi(x+L)=\psi(x) \tag{2.17}$$

and the corresponding conditions in the other directions leads to discrete values of $k$ according to

$$\psi(x+L)=e^{ikx}e^{ikL}=e^{ikx}\Rightarrow k=\pm n_x\frac{2\pi}{L} \tag{2.18}$$

where $n_x$ is an integer.
The electron energy grows quadratically with $k$ according to

$$E=\frac{\hbar^2k^2}{2m} \tag{2.19}$$

with no directional dependence in $k$-space. The allowed $k$-points are illustrated in 2 dimensions on Fig. 2.7. Each $k$-point contains 2 electrons of opposite spin and these states are filled from the lowest energy (smallest $k$) until all electrons are used. The highest energy is called the Fermi energy $E_F$ and the corresponding radius $k_F$. This radius separates occupied and unoccupied levels. One state occupies $(2\pi/L)^3$ in $k$-space. The number of electrons $N$ inside a spere with radius $k$ is

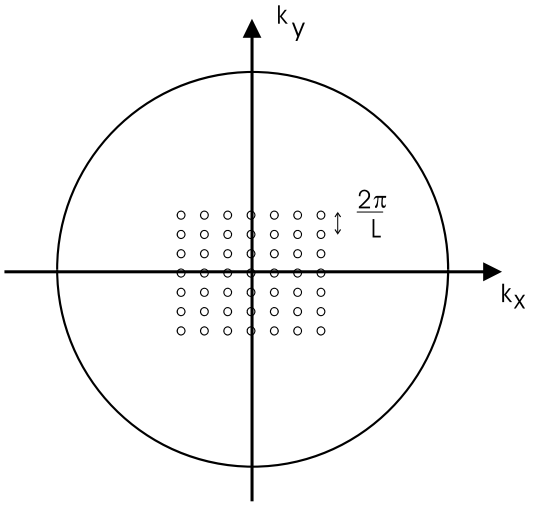

Fig. 2.7. Allowed k-points in 2 dimensions

$$N=2\frac{4\pi k^3/3}{(2\pi/L)^3}=\frac{V}{3\pi^3}k^3. \tag{2.20}$$

By inserting $k=\left(\frac{2mE}{\hbar^2}\right)^{1/2}$ we get the density of states – the number of states per energy unit:

$$D(E)=\frac{dN}{dE}=\frac{d}{dE}\left[\frac{V}{3\pi^2}\left(\frac{2mE}{\hbar^2}\right)^{3/2}\right]=\frac{V}{2\pi^2}\left(\frac{2m}{\hbar^2}\right)^{3/2}E^{1/2}. \tag{2.21}$$

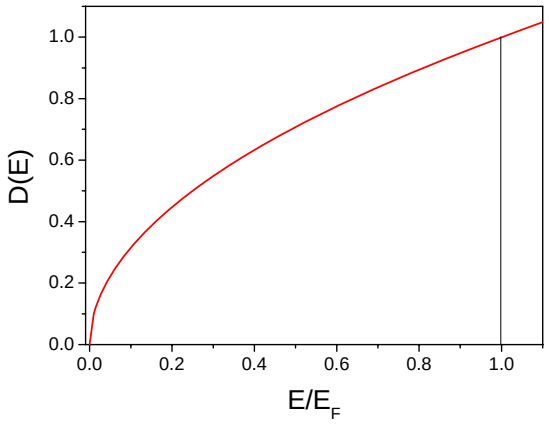

Fig. 2.8. Free electron density of states.

## 2.3 Density of states in two dimensions

The 2D density of states must reflect the quantization of levels described in the previous section. Consider a slab of material that has macroscopic dimensions in the $x$- and $y$-directions while the thickness is small (in the nanometer range). Periodic boundary conditions in the $x$- and $y$- directions lead to

$k_x = \frac{n2\pi}{L_x}$, $k_y = \frac{l2\pi}{L_y}$, $n,l = 1,2,3,\cdots$ . The area per *k*-point in *k*-space is then

$$S_k = \frac{4\pi^2}{L_x L_y} = \frac{4\pi^2}{S}. \tag{2.22}$$

The number of states within a circle with radius *k* is then

$$N(k) = 2\,\frac{\pi k^2}{4\pi^2/S} = \frac{k^2 S}{2\pi} \tag{2.23}$$

where the factor 2 is due to spins. The number of states between *k* and *dk* is given by

$$\rho(k) = \frac{dN}{dk}dk = \frac{k}{\pi}S\,dk\,. \tag{2.24}$$

Similarly, the number of states between *E* and *E*+*dE* is calculated from

$$\frac{dN}{dE}dE = \frac{dN}{dk}\frac{dk}{dE}dE\,. \tag{2.25}$$

The number of states per area and per energy unit is then given by

$$\frac{1}{S}\frac{dN(E)}{dE} = \frac{k}{\pi}\frac{dk}{dE}. \tag{2.26}$$

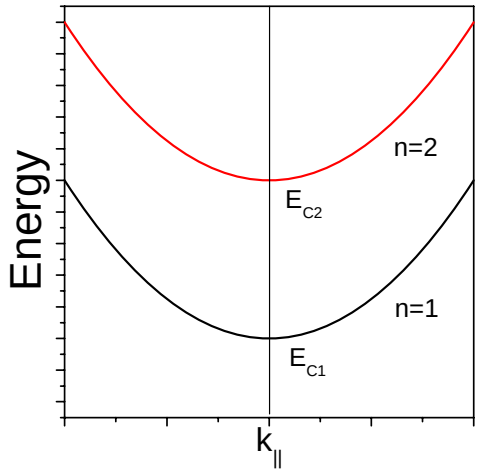


Fig. 2.9. Energy bands as a function of $k_{||}$.

Using the form of the free electron energy to get the relation $\frac{dk}{dE} = \frac{1}{2\hbar}\sqrt{\frac{2m}{E}}$ the 2D density of states take the form

$$\rho_{2D}(E) = \frac{1}{S}\frac{dN}{dE} = \frac{k}{\pi}\frac{dk}{dE} = \frac{m}{\hbar^2\pi}. \tag{2.27}$$

It is important to notice that the 2D density of states is independent of the energy. However, ρ depends on the number of levels and is thus a sum of the contributions from the discrete levels appearing as a result of the quantization

$$\rho_{2D} = \sum_{n=1}^{\infty}\frac{m}{\hbar^2\pi}H\left(E - E_{cn}\right) \tag{2.28}$$

where $H(E\text{-}E_{cn})$ is the Heaviside step function and $E_{cn}$ denotes the conduction band minima of the discrete levels.

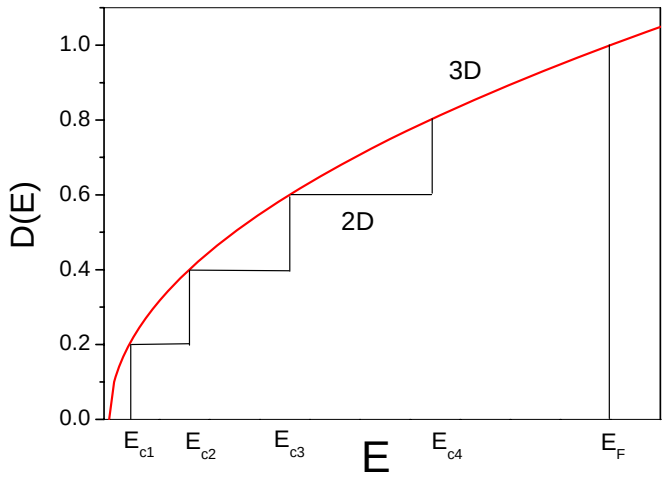


Fig. 2.10. Density of states for a 2D system.

## 2.4 One-dimensional systems

Systems where electrons are free to move in one direction and confined in the other two directions are investigated intensively these years. A large number of different structures have been grown and a wide range of interesting applications have been suggested, including electronic components, sensors, and light emitting components (lasers).

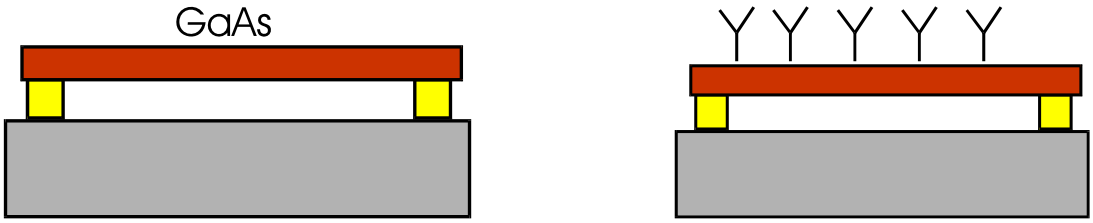


Fig. 2.11. Schematic illustration of a wire placed on top of two contacts. In figure b) the y's signify molecular acceptors placed on the wire in order to make it sensitive to specific molecules. If the wire is very thin a few molecules will be enough to induce a measurable change in resistivity of the wire.

Figure 2.12 shows a structure consisting of GaAs wire with rectangular cross section surrounded by AlGaAs. In the following this will be treated as a system with electronic confinement in the *y*- and *z*-directions and free electron motion in the *x*-direction. The Schrödinger equation takes the form

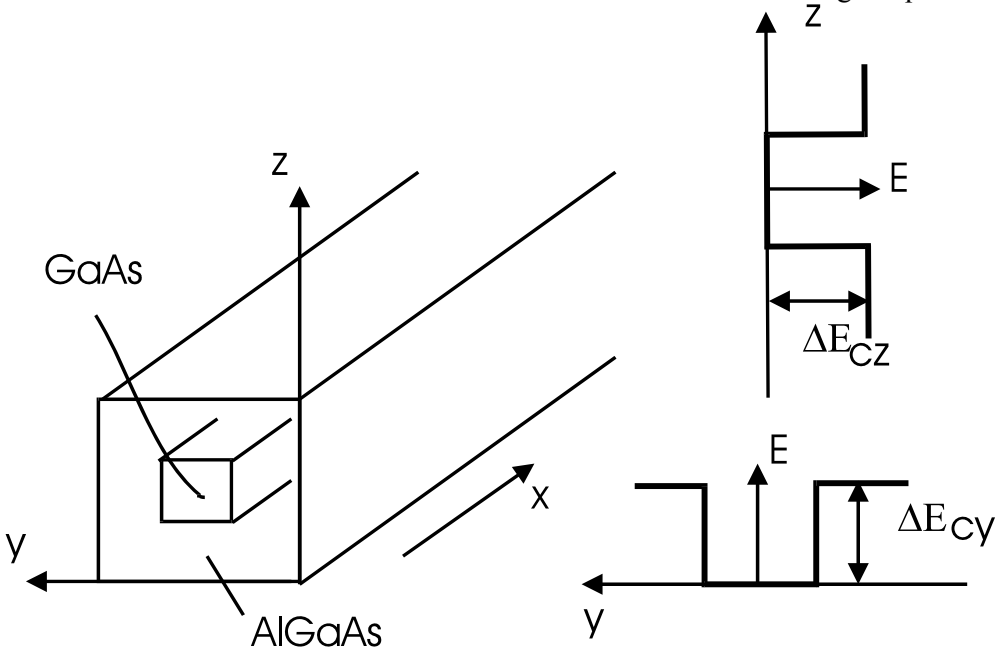


Fig. 2.12. A nanowire with rectangular cross section along with the potentials in two directions.

$$\left[\frac{p_x^2+p_y^2+p_z^2}{2m}+V(y,z)\right]\Psi(x,y,z)=\Psi(x,y,z)E \tag{2.29}$$

where the potential in the *x*- and *y*-directions are illustrated in Figure 2.12. Assuming free movement in the x-direction independent of the other two coordinates leads to a solution of the form

$$\Psi(x,y,z)=\frac{1}{\sqrt{L_x}}\phi(y,z)\,e^{ik_x x}. \tag{2.30}$$

In general *y* and *z* can not be separated for finite barriers and the Schrödinger equation

$$\left[\frac{p_y^2+p_z^2}{2m}+V(y,z)\right]\phi(x,y,z)=\phi(x,y,z)E \tag{2.31}$$

is more difficult to solve than for the QW case treated earlier. If we assume infinite barriers the solution will be standing waves of the form

$$\phi(y,z)=\frac{2}{\sqrt{L_yL_z}}\cos\left(\frac{n_y\pi\,y}{L_y}\right)\cos\left(\frac{n_z\pi\,z}{L_z}\right),\qquad n_y,n_z=1,2,3,\cdots \tag{2.32}$$

where $\phi$=0 on the boundaries and $k_{y,z}=\frac{n_{y,z}\pi}{L_{y,z}}$. Inserting this in the Schrödinger equation with *V*=0 gives discrete energies

$$E_{n_y,n_z}=\frac{\hbar^2\pi^2}{2m}\left(\frac{n_y^2}{L_y^2}+\frac{n_z^2}{L_z^2}\right). \tag{2.33}$$

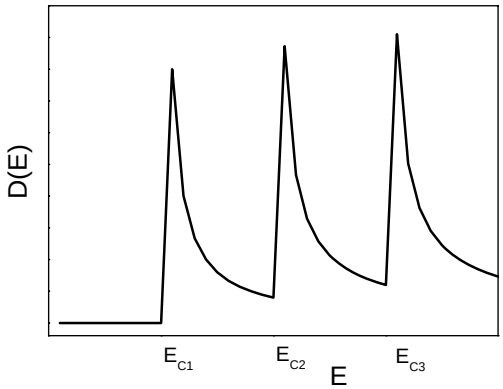

Fig. 2.13 Density of states of a 1D system.

Along the *x*-axis the electrons are free to move and the total energy is

$$E=\frac{\hbar^2\pi^2}{2m}\left(\frac{n_y^2}{L_y^2}+\frac{n_z^2}{L_z^2}\right)+\frac{\hbar^2k_x^2}{2m}. \tag{2.34}$$

The density of states is calculated along the same line as for the quantum well

$$D_i(E)=\frac{L_x}{\pi\hbar}\sqrt{\frac{m_e}{2(E-E_i)}}. \tag{2.35}$$

In this simple model $D(E)\to\infty$ for $E=E_i$.

Exercise: Start with a simple quantum well with infinite barriers, introduce constraints on electron motion in one more direction. How much does the lowest energy shift? Take a 10 nm thick GaAs QW as example. The effective mass in the conduction band is 0.067 times the free-electron mass.

Exercise: Consider a Ag quantum well with infinite barriers. How many levels are there below the Fermi energy if the well is 1 nm thick? Use $E_F$=5.48 eV (1 eV=1.6×10$^{-19}$ J, $\hbar$=1.05×10$^{-34}$ Js).

## 2.5 Zero-dimensional systems

Following the line of the previous sections we should now move down to 0D systems where the electrons are confined in their motion in all three directions. Various names appear for that type of systems such as quantum dots, quantum boxes, nano crystals etc.

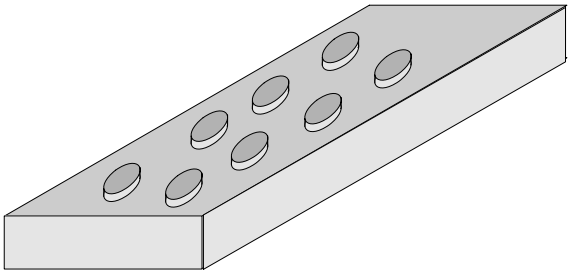

Fig. 2.14. Lattice of cylindrical structures produced on a surface, for instance by e-beam lithography. In general the effective diameter will be smaller than the physical diameter due to the existence of localized surface states.

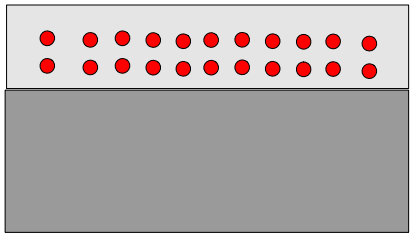

Fig. 2.15. Nano particles embedded in a matrix material, for instance semiconductor nanocrystals in silicon dioxide.

Consider a quantum box with infinite barriers and side lengths $L_x$, $L_y$, $L_z$. The wave function will have the form

$$\phi_{lmn} = \phi_l(x)\phi_m(y)\phi_n(z) \tag{2.36}$$

with solutions in the form of standing waves

$$\phi_l(x) = \sqrt{\frac{2}{L_x}}\sin\left(k_x x\right). \tag{2.37}$$

The energy is given by

$$E_{lmn} = E_g + E_{xl} + E_{ym} + E_{zn} \tag{2.38}$$

with

$$E_{xl} = \frac{\hbar^2 k_x^2}{2m} = \frac{\hbar^2}{2m}\left(\frac{\pi}{L_x}\right)^2 l^2. \tag{2.39}$$

These discrete energy levels now describe the total energy of the system and no continuous part from free electron movements should be added as in the 1D and 2D cases. In this sense the system appears as an artificial atom. The density of states can thus be written up directly

$$\rho^{0D}(E) = 2\sum_{lmn}\delta\left(E - E_{lmn}\right). \tag{2.40}$$

Consider a cube with side length $a$. The energies are then

$$E_n = \frac{\hbar^2}{2m_e}\left(\frac{\pi}{a}\right)^2 n^2, \qquad n^2 = \sum_i n_i^2, \ \ i = 1,2,3,\cdots. \tag{2.41}$$

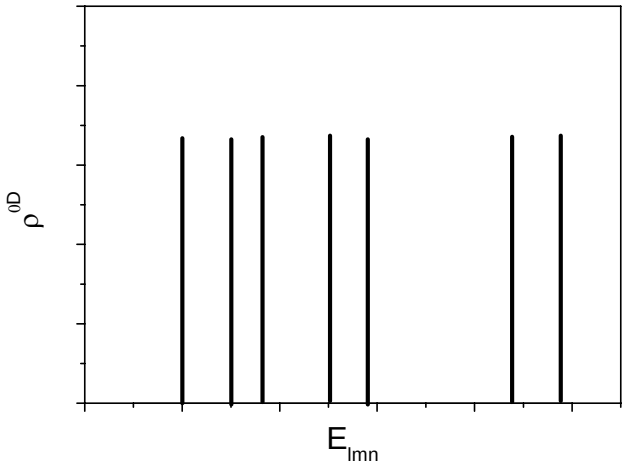


Fig. 2.15. Density of states for a 0D system.

The lowest value is $n^2=1^2+1^2+1^2$. The corresponding energies for holes are given by

$$E_h = \frac{\hbar^2}{2m_h}\left(\frac{\pi}{a}\right)^2 n^2 . \qquad (2.42)$$

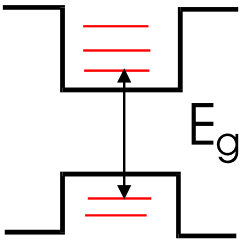


Fig. 2.17. Electron and hole states in the quantum dot.

Due to the quantzation the energy gap increases compared to bulk material. Taking both electrons and holes into account the increase in gap energy is given by

$$\Delta E_g = \frac{\hbar^2}{2\mu}\left(\frac{\pi}{a}\right)^2 n^2 \qquad (2.43)$$

where $\frac{1}{\mu} = \frac{1}{m_e} + \frac{1}{m_h}$ is the reduced mass. For 10-nm GaAs quantum boxes the change in gap energy is 0.2 eV.

**Exercise:** If the quantum box is very small there will not be confined levels in the box. What is the condition for at least one bound level?

$$\Delta E_C > \frac{\hbar^2 k^2}{2m_e}$$

with $k = k_{\min} = \left(\frac{\pi}{a}\right)^2 n^2,\ \ n^2 = 3$.

This gives

$$\Delta E_C > \frac{\hbar^2}{2m_e}\left(\frac{\pi}{a}\right)^2 3$$

and then

$$a^2 > \frac{3\hbar^2\pi^2}{2m_e\,\Delta E_C}.$$

For $Al_{0.3}Ga_{0.7}As$ the dept of the confining potential $\Delta E_C = 230meV$ corresponding to a minimum size of the box $a$=2.2 nm.

## 3. **Optical properties – Interband transitions**

Some of the most useful techniques for studies of the properties of nanostructures are based on the optical transitions between the discrete electronic levels. Absorption spectroscopy, for instance, will reveal the direct band gap and thereby also an increase in gap energy (blue shift) due to confinement effects.

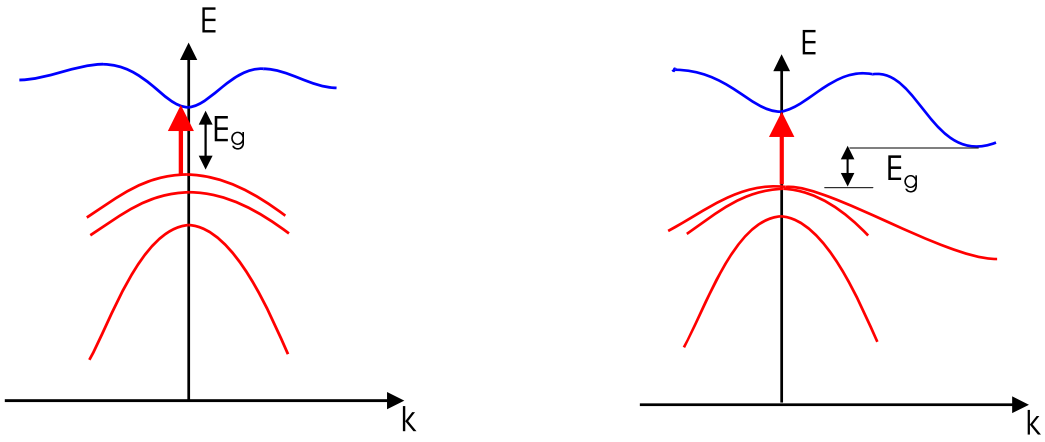


Fig. 3.1. Direct (left) and indirect (right) band gaps. This could for instance be GaAs (left) and Si (right).

Figure 3.1 above illustrates two situations that occur in symmetry directions in semiconductors. If the highest point in the (occupied) valence band lies directly under the lowest point in the (empty) conduction band we talk about a direct band gap and the gap energy corresponds to the onset of optical absorption. If, on the other hand, maxima and minima in the valence and conduction band appear at different points in *k*-space we talk about an indirect gap. Since optical transitions are vertical in the *E(k)* diagram the absorption at the indirect gap will be weak and transitions at the direct gap will dominate the absorption spectrum.

The transition rate from initial (i) to final (f) state is given by

$$W_{i\to f} = \frac{2\pi}{\hbar}|M|^2 g(\hbar\omega) \qquad (3.1)$$

where the matrix element is given by

$$M = \int \psi_f^* H'(\vec{r})\psi_i d\vec{r} \qquad (3.2)$$

and $g(\hbar\omega)$ is the joint density of states which is a folding of the density of states of the initial and final states. In order to calculate the transition matrix element an expression for the interaction Hamiltonian *H'* is needed. In classical physics the energy of an atom considered as a dipole in an electric field $\vec{\varepsilon}$ is $E = -\vec{p}\cdot\vec{\varepsilon}$. As a first approximation we can then use that to express the interaction Hmiltonian on the form $H' = +e\vec{r}\cdot\vec{\varepsilon}$. Let us consider a plane wave of the form

$$\vec{\varepsilon}(\vec{r}) = \vec{\varepsilon}_0 e^{i\vec{k}\cdot\vec{r}} \qquad (3.3)$$

and electronic wavefunction on the Bloch form

$$\psi_{i,f}(\vec{r}) = \frac{1}{\sqrt{V}} u_{i,f}(\vec{r}) e^{i\vec{k}_{i,f}\cdot\vec{r}} \qquad (3.4)$$

where the functions $u_{i,f}(\vec{r}+\vec{T}) = u_{i,f}(\vec{r})$ are periodic in the crystal lattice described by translation vectors $\vec{T}$. With this we get

$$M = \frac{e}{V}\int u_f^*(\vec{r}) e^{-i\vec{k}_f\cdot\vec{r}} \left(\vec{\varepsilon}_0 \cdot \vec{r} e^{i\vec{k}\cdot\vec{r}}\right) u_i(\vec{r}) e^{i\vec{k}_i\cdot\vec{r}} d\vec{r} \qquad (3.5)$$

which by using the momentum conservation $\hbar\vec{k} = \hbar\vec{k}_f - \hbar\vec{k}_i$ is reduced to

$$M = \frac{e}{V}\int u_f^*(\vec{r})\left(\vec{\varepsilon}_0 \cdot \vec{r}\right) u_i(\vec{r}) d\vec{r}\,. \qquad (3.6)$$

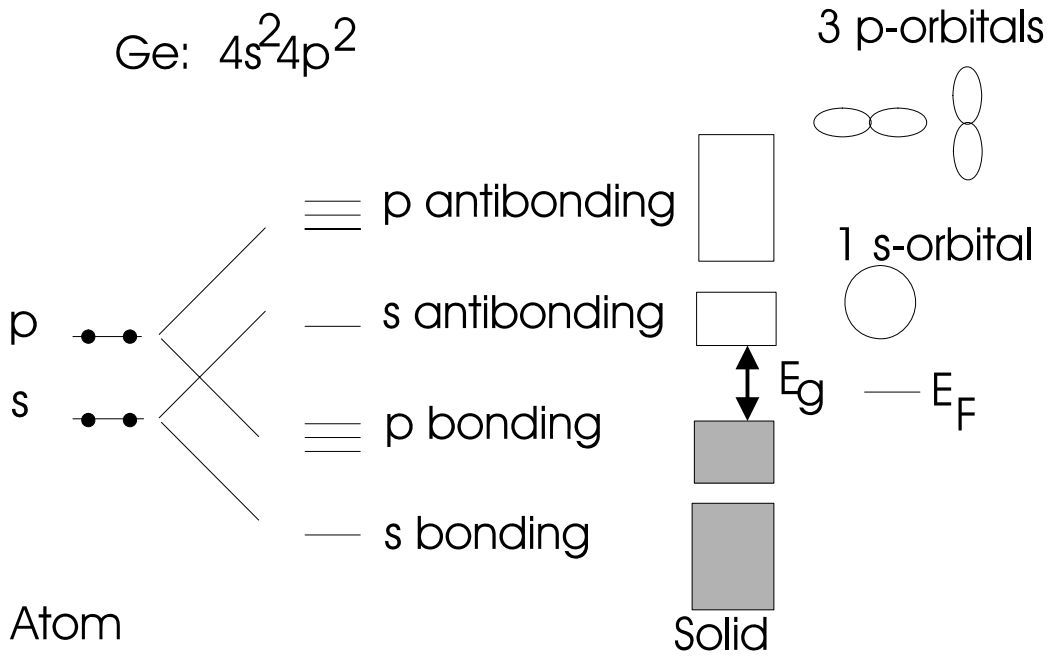


Figure 3.2. The transition from free atoms to atoms with bonds in a solid.

The transition matrix element thus only depends on the space coordinate through the cell-periodic part of the Bloch function. These functions also contain the dependence on the material. The calculation of *M* can thus be done through integration over a single Brillouin cell.
In order to continue the evaluation of the optical transition rate we need to consider the symmetry of wave functions in solids. Figure 3.2 illustrates the transition from discrete atomic levels to continuous bands of levels in Ge.

The scheme shown in Fig. 3.2 is in principle the same for III-V alloys such as GaAs or II-VI alloys like CdTe. It is found that the transition matrix element is large for p →s transitions, for instance from the valence band to the conduction band of semiconductors.
Near the band edge (Fig. 3.3) the 4 bands of a semiconductor are parabolic with the form

$$E = \frac{\hbar^2 k^2}{2m^*} \qquad (3.7)$$

where *m** is the effective mass describing the curvature of the individual bands as can be seen from

$$\frac{d^2E}{dk^2} = \frac{\hbar^2}{m^*} \Rightarrow \frac{1}{m^*} = \frac{1}{\hbar^2}\frac{d^2E}{dk^2}. \qquad (3.8)$$

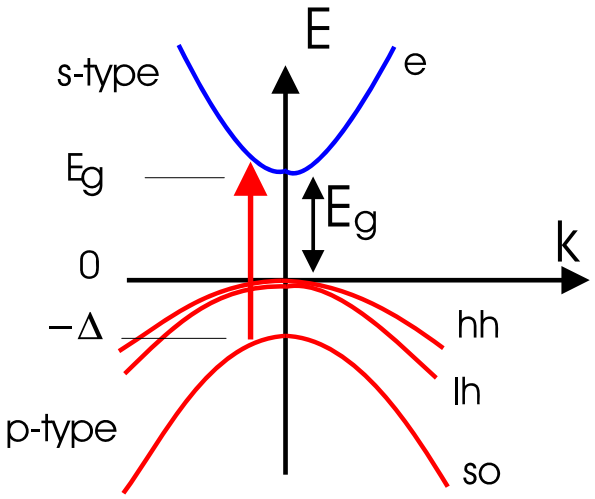


Fig. 3.3. The band near teh band gap in a semiconductor.

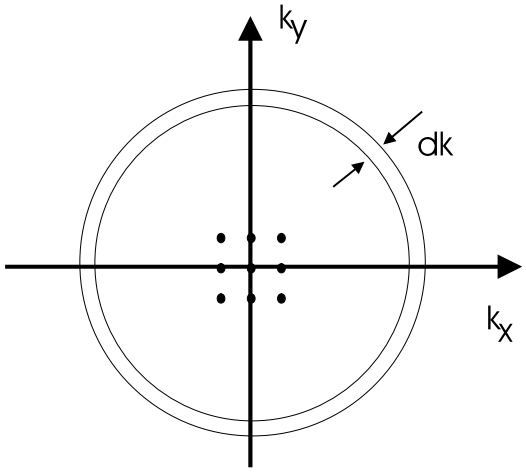


Fig. 3.4. The discrete values of the k-vector in reciprocal space.

From Fig. 3.4 it can be seen that $g(k) = \frac{1}{(2\pi)^3} 4\pi k^2 = k^2 \Big/ 2\pi^2$ where as before $\frac{1}{(2\pi)^3}$ is the number of k-points per unit volume. The relation to the density of states per energy unit is seen from

$$2g(k)dk = g(E)dE \Rightarrow g(E) = \frac{2g(k)}{dE \Big/ dk}. \qquad (3.9)$$

Inserting the expression for g(k) and using the parabolic form *E(k)* described above we arrive at

$$g(E) = \frac{1}{2\pi^2}\left(\frac{2m^*}{\hbar^2}\right)^{3/2}\sqrt{E}. \qquad (3.10)$$

We will consider transitions between the bands

$$E_c(k) = E_g + \frac{\hbar^2 k^2}{2m_e}$$
$$E_h(k) = -\frac{\hbar^2 k^2}{2m_h} \qquad (3.11)$$

which gives a difference in energy between the two bands of the form

$$\hbar\omega = E_g + \frac{\hbar^2 k^2}{2m_e} + \frac{\hbar^2 k^2}{2m_h} = E_g + \frac{\hbar^2 k^2}{2\mu}, \qquad \frac{1}{\mu} = \frac{1}{m_e} + \frac{1}{m_h}. \qquad (3.12)$$

To get an expression for the joint density of states we thus just have to replace the effective mass by the reduced mass in Eq. (3.10) above

$$\hbar\omega < E_g : \; g(\hbar\omega) = 0$$
$$\hbar\omega \geq E_g : \; g(E) = \frac{1}{2\pi^2}\left(\frac{2\mu}{\hbar^2}\right)^{3/2}\sqrt{\hbar\omega - E_g}. \qquad (3.13)$$

Since the absorption is proportional to the transition rate we have

$$\alpha(\hbar\omega) \propto |M|^2 g(\hbar\omega). \qquad (3.14)$$

As $M$ is a number the spectral dependence of the absorption is given by the joint density of states. Similar arguments apply to low-dimensional structures. Below the forms of absorption spectra from different systems are sketched.

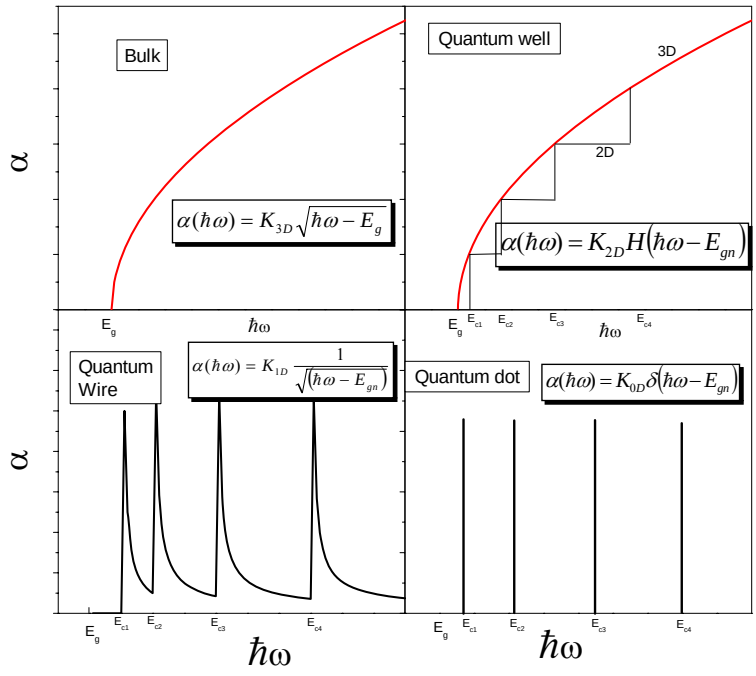


Fig. 3.5. Density of states in different systems.

## 4. **Hybridization of carbon atoms**

Carbon atoms are the basic building blocks of organic (soft) materials. At the same time they form diamond, the hardest known material, when they are arranged in the diamond crystal structure. The properties of carbon structures are strongly connected to the many different configurations of the electronic stats of carbon atoms usually referred to as the hybridization. Carbon atoms have 6 electrons occupying $1s^2$, $2s^2$, and $2p^2$ orbitals. The four *2s* and *2p* valence electrons form covalent bonds, for instance in the diamond structure where each atom has 4 nearest neighbours. However, the energy difference between the lowest *2s* electron and the highest *2p* electron is quite small, which leads to easy mixing of orbitals and formation of hybridizations of a *2s* electron with 1, 2, or 3 *2p* electrons: *sp*, $sp^2$, $sp^3$.

Let us first consider sp hybridization where a *2s* state is combined with a $2p_x$ state in order to describe bonding between two atoms laying on the *x*-axis. As illustrated in Fig. 4.1 there is two possible combinations described by

$$\begin{aligned} |sp_a\rangle &= C_1|2s\rangle + C_2|2p_x\rangle \\ |sp_b\rangle &= C_3|2s\rangle - C_4|2p_x\rangle. \end{aligned} \qquad (4.1)$$

Orthonormalization requires

$$\begin{aligned} \langle sp_a \| sp_b\rangle &= 0 \\ \langle sp_a \| sp_a\rangle &= \langle sp_b \| sp_b\rangle = 1, \end{aligned} \qquad (4.2)$$

which leads to

$$\begin{aligned} |sp_a\rangle &= \frac{1}{\sqrt{2}}\left(|2s\rangle + |2p_x\rangle\right) \\ |sp_b\rangle &= \frac{1}{\sqrt{2}}\left(|2s\rangle - |2p_x\rangle\right). \end{aligned} \qquad (4.3)$$

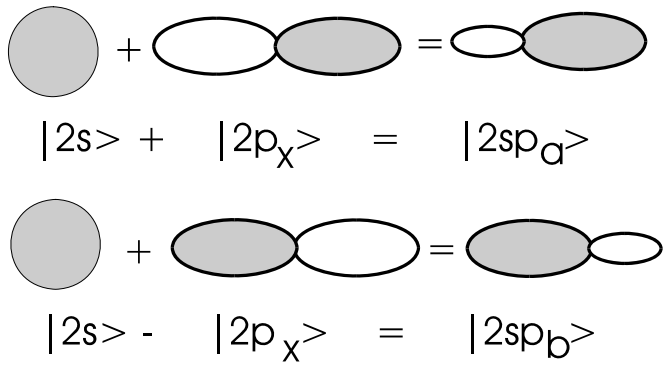


Fig. 4.1. Hybridization of 2*s* and 2*p* states.

The same considerations holds for the *y*- and *z*-directions. Mixing of *2p* orbitals with each other gives rise to rotation of the resulting orbital. A wavefunction

$$|2p_a\rangle = C_x|2p_x\rangle + C_y|2p_y\rangle + C_z|2p_z\rangle \qquad (4.4)$$

where $C_x^2 + C_y^2 + C_z^2 = 1$ corresponds to a 2p wavefunction describing a bond in the direction $(C_x,C_y,C_z)$.

A simple example of a molecule containing carbon atoms showing *sp* hybridization is acetylene $C_2H_2$ with triple bonds between carbon atoms often represented by HC≡CH. In this linear molecule the $|sp_a\rangle$ orbital of one C atom forms a covalent bond with the $|sp_b\rangle$ orbital of the other C atom. This is called a σ bond and as it is usually the case with covalent bonds it is rather strong. Two much weaker so called π bonds are formed by the remaining $2p_y$ and $2p_z$ wavefunctions.

Polyacetylene is a well-known semiconducting polymer that can appear with different structures. All of them contain however $sp^2$ hybridized bonds. In $sp^2$ hybridization a *2s* orbital is combined with two *2p* orbitals, for instance $2p_x$ and $2p_y$. This forms the strong σ bonds of the polymer chain. The last *2p* bond forms weak π bonds in the direction perpendicular to the plane of the molecule. The combination of two *2p* bonds in the hybridization leads to the zig-zag structure of the chain.

The σ bonds point in the directions

$$(0,-1,0),\ \left(\sqrt{3}/2,\ 1/2,0\right),\ \left(-\sqrt{3}/2,\ 1/2,0\right). \tag{4.5}$$

The $\left|sp_i^2\right\rangle$ states are formed from *2s*, $2p_x$, and $2p_y$ atomic levels with the normalization condition

$$\left\langle sp_i^2 \middle| sp_i^2 \right\rangle = 1. \tag{4.6}$$

Using this the 3 bonds in the directions given above can be represented by

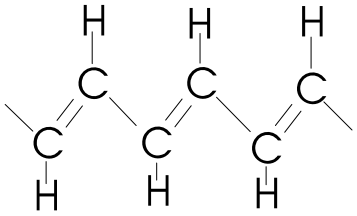

$$\begin{aligned}
\left|sp_a^2\right\rangle &= c_1\left|2s\right\rangle - \sqrt{1-c_1^2}\left|2p_y\right\rangle \\
\left|sp_b^2\right\rangle &= c_2\left|2s\right\rangle + \sqrt{1-c_2^2}\left[\sqrt{3}/2\left|2p_x\right\rangle + ½\left|2p_y\right\rangle\right] \\
\left|sp_c^2\right\rangle &= c_3\left|2s\right\rangle + \sqrt{1-c_3^2}\left[-\sqrt{3}/2\left|2p_x\right\rangle + ½\left|2p_y\right\rangle\right].
\end{aligned} \tag{4.7}$$

Fig. 4.2. Polyacetylene.

Distribution of the *2s*-part (othonormalization) requires that $c_1^2 + c_2^2 + c_3^2 = 1$. The following conditions lead us to the $c_i$ coefficients

$$\begin{aligned}
&\left\langle sp_a^2 \middle| sp_b^2 \right\rangle = 0 \ \Rightarrow\ c_1c_2 - ½\sqrt{1-c_1^2}\sqrt{1-c_2^2} = 0 \\
&\left\langle sp_a^2 \middle| sp_c^2 \right\rangle = 0 \ \Rightarrow\ c_1c_3 - ½\sqrt{1-c_1^2}\sqrt{1-c_3^2} = 0 \\
&\Rightarrow c_1 = c_2 = 1/\sqrt{3},\quad c_3 = -1/\sqrt{3}.
\end{aligned} \tag{4.8}$$

This gives then the linear combination of the atomic orbitals that can be described as triangular bonds with the largest amplitude along the directions to the nearest neighbours.

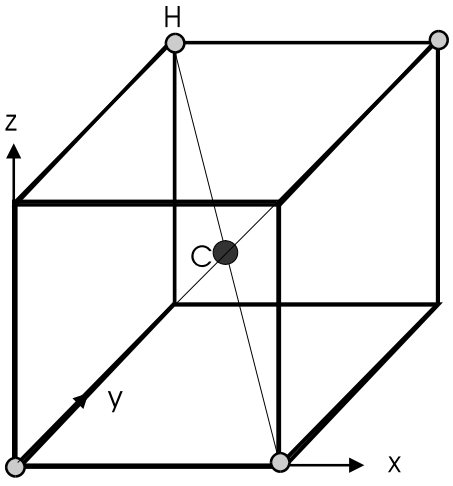


Fig. 4.3. Position of C atoms in $CH_4$.

As examples of $sp^3$ hybridization we will consider Alkenes ($C_nH_{2n+2}$) and in particular the Methan molecule $CH_4$. In this case the *2s* state is mixed with 3 *2p* states. The directions of the bonds are given by (1,1,1), (-1,-1,1), (-1,1,-1), and (1,-1,-1) and the combination of orbitals can be written up directly:

$$\begin{aligned}
\left|sp_a^3\right\rangle &= ½\left[\left|2s\right\rangle + \left|2p_x\right\rangle + \left|2p_y\right\rangle + \left|2p_z\right\rangle\right] \\
\left|sp_b^3\right\rangle &= ½\left[\left|2s\right\rangle - \left|2p_x\right\rangle - \left|2p_y\right\rangle + \left|2p_z\right\rangle\right] \\
\left|sp_c^3\right\rangle &= ½\left[\left|2s\right\rangle - \left|2p_x\right\rangle + \left|2p_y\right\rangle - \left|2p_z\right\rangle\right] \\
\left|sp_d^3\right\rangle &= ½\left[\left|2s\right\rangle + \left|2p_x\right\rangle - \left|2p_y\right\rangle - \left|2p_z\right\rangle\right].
\end{aligned} \tag{4.9}$$

In general for $sp^n$ hybridization we have: $\begin{matrix} n+1 \ electrons \ in \ \sigma \ orbitals \\ 4-(n+1) \ electrons \ in \ \pi \ orbitals \end{matrix}$. (4.10)

Thus we have: $\begin{matrix} sp & : 2\sigma + 2\pi \\ sp^2 & : 3\sigma + 1\pi \\ sp^3 & : 4\sigma + 0\pi \end{matrix}$ . (4.11)

**Exercise**: Derive the expressions for the coefficients $c_1$, $c_2$ and $c_3$ for the $sp^2$ hybridization.

## 5. **Tight-binding calculations**

Consider a crystalline material with a periodic lattice. The wavefunctions $\Psi(\vec{r})$ are Bloch functions fulfilling the condition

$$T_{\vec{a}_i}\,\psi = e^{i\vec{k}\cdot\vec{a}_i}\psi \tag{5.1}$$

which also can be expressed as

$$\psi(\vec{r}+\vec{a}_i) = e^{i\vec{k}\cdot\vec{a}_i}\psi(\vec{r})\,. \tag{5.2}$$

Here $T_{\vec{a}_i}$ is a translational operator and $\vec{a}$ is a lattice vector.

We will take atomic orbitals as the starting point and construct a function that satifies the Bloch condition:

$$\Phi_j(\vec{k},\vec{r}) = \frac{1}{\sqrt{N}}\sum_{\vec{R}}^{N} e^{i\vec{k}\cdot\vec{R}}\phi(\vec{r}-\vec{R}),\ \ j=1,2,\cdots,n \tag{5.3}$$

where

$\vec{R}$ : *position of atoms*

$\phi_j$ : *atomic wavefunction,* $j^{th}$ *state*

$n$ : *number of atomic orbitals in unit cell*

$N$ : *number of unit cells* ($\sim 10^{24}$).

Usually *n* is a small number. The form in Eq. (5.3) satisfies the Bloch condition:

$$\begin{aligned}\Phi_j(\vec{k},\vec{r}+\vec{a}) &= \frac{1}{\sqrt{N}}\sum_{\vec{R}}^{N} e^{i\vec{k}\cdot\vec{R}}\phi(\vec{r}+\vec{a}-\vec{R}) \\ &= e^{i\vec{k}\cdot\vec{a}}\,\frac{1}{\sqrt{N}}\sum_{\vec{R}-\vec{a}}^{N} e^{i\vec{k}\cdot(\vec{R}-\vec{a})}\phi_j(\vec{r}-(\vec{R}-\vec{a})) \\ &= e^{i\vec{k}\cdot\vec{a}}\Phi_j(\vec{k},\vec{r}).\end{aligned} \tag{5.4}$$

The last step in Eq. (5.4) follows by realizing that subtracting a lattice vector from the atomic position vector just changes the order of the summation.

Let us consider periodic boundary conditions of the form

$$\Phi_j(\vec{k},\vec{r}+M\vec{a}_i) = \Phi_j(\vec{k},\vec{r}),\quad i=1,2,3 \qquad M\equiv N^{1/3}. \tag{5.5}$$

Using this boundary condition together with the Bloch condition in Eq. (4) gives us discrete values of the wavevector *k*.

$$e^{ikMa_i} = 1 \Rightarrow k = \frac{2p\pi}{Ma_i},\ p=0,1,\cdots,M-1 \qquad i=1,2,3\,. \tag{5.6}$$

Let us now write the wavefunction in the solid material as a superposition of the functions in Eq. (5.3):

$$\psi_j(\vec{k},\vec{r}) = \sum_{j'=1}^{n} c_{jj'}(\vec{k})\Phi_{j'}(\vec{k},\vec{r})\,. \tag{5.7}$$

Since (5.3) satisfies Blochs theorem so does the sum in (5.7).

The energy eiegnvalues are given by

$$\vec{E}j(\vec{k}) = \frac{\langle \psi_j | H | \psi_j \rangle}{\langle \psi_j | \psi_j \rangle} \tag{5.8}$$

where H is the Hamilton operator. By inserting the form in (5.7) we get

$$E_i(k) = \frac{\sum_{j,j'=1}^{n} H_{jj'}(k) c_{ij}^* c_{ij'}}{\sum_{j,j'=1}^{n} S_{jj'}(k) c_{ij}^* c_{ij'}} \tag{5.9}$$

where

$H_{jj'} = \langle \Phi_j | H | \Phi_{j'} \rangle$

$S_{jj'} = \langle \Phi_j | \Phi_{j'} \rangle$

are the transition matrix elements and overlap matrix elements, respectively. For given $n \times n$ matrices ($H_{jj'}$ and $\rho_{jj'}$) and given $\vec{k}$ we should determine $c_{ij}$ such that the energy $E_i$ is minimized. The condition is (remembering that $c_{ij}$ is complex)

$$\frac{\partial E_i(\vec{k})}{\partial c_{ij}^*} = \frac{\sum_{j'=1}^{n} H_{jj'}(\vec{k}) c_{ij'}}{\sum_{j,j'=1}^{n} S_{jj'}(\vec{k}) c_{ij}^* c_{ij'}} - \frac{\sum_{j,j'=1}^{n} H_{jj'}(\vec{k}) c_{ij}^* c_{ij'}}{\left( \sum_{j,j'=1}^{n} S_{jj'}(\vec{k}) c_{ij}^* c_{ij'} \right)^2} \sum_{j'=1}^{n} S_{jj'}(\vec{k}) c_{ij'} = 0 . \tag{5.10}$$

If we multiply by $\sum S_{jj'}(\vec{k}) c_{ij}^* c_{ij'}$ and use the expression for $E$ in (5.9) we get

$$\sum H_{jj'}(\vec{k}) c_{ij} = E_i(\vec{k}) \sum S_{jj'}(\vec{k}) c_{ij'} . \tag{5.11}$$

By defining

$$C_i = \begin{pmatrix} c_{i1} \\ . \\ . \\ c_{in} \end{pmatrix} \tag{5.12}$$

We can get the following algebraic set of equations

$$\begin{aligned} &\vec{\vec{H}} C_i = E_i(\vec{k}) \vec{\vec{S}} C_i \\ &or \\ &\left[ \vec{\vec{H}} - E_i \vec{\vec{S}} \right] C_i = 0. \end{aligned} \tag{5.13}$$

The condition for solutions is

$$Det\left[ \vec{\vec{H}} - E_i \vec{\vec{S}} \right] = 0 . \tag{5.14}$$

This is an eigenvalue problem with $n$ eigenvales for each $\vec{k}$ .

The procedure leading to calculations of energy levels is the following:

1. Determine unit cell and basis, lattice vectors $\vec{a}_i$

2. Reciprocal lattice $\vec{b}_i$
3. Chose symmetry directions, calculate $H_{ij}$ , $S_{ij}$
4. Solve $\left[\vec{H} - E_i \vec{S}\right] C_i = 0$ in order to find $E_i(\vec{k})$, $c_{ij}(\vec{k})$.

It should be noted that this is not a self consistent procedure. The result depends completely on the initial choice of atomic wavefunctions.

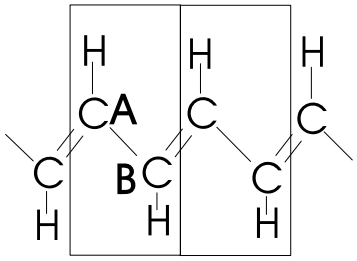


As an example we calculate the electronic bands of Polyacetylene. The unit cell is shown on Fig. 5.1. The molecule can be treated as a one-dimensional system with two C atoms A and B in the unit cell. Thus $\vec{a}_1 = (a,0,0)$ and $\vec{b}_1 = \left(\frac{a}{2\pi},0,0\right)$, and the Brillouin zone is given by $-\pi/a < k < \pi/a$.

Fig. 5.1. Unit cells in polyacetylene.

The sum over atomic wavefunctions runs over the two different atoms A and B:

$$\Phi_j(r) = \frac{1}{\sqrt{N}} \sum_{\vec{R}_\alpha} e^{i\vec{k}\cdot\vec{R}_\alpha} \phi(\vec{r} - \vec{R}_\alpha), \qquad \alpha = A, B. \tag{5.15}$$

The diagonal matrix element is given by

$$\begin{aligned} H_{AA}(\vec{r}) &= \frac{1}{N} \int \sum_{R'} e^{-ikR'} \phi_A^*(r - R') H \sum_R e^{ikR} \phi(r - R)\, dV \\ &= \frac{1}{N} \sum_{R,R'} e^{ik(R-R')} \left\langle \phi_A^*(r - R') \middle| H \middle| \phi_A(r - R) \right\rangle \\ &= \frac{1}{N} \sum_{R=R'} \left\langle \phi_A^*(r - R) \middle| H \middle| \phi_A(r - R) \right\rangle \\ &= \frac{1}{N} \sum_{R=R'\pm a'} e^{\pm ika} \left\langle \phi_A^*(r - R') \middle| H \middle| \phi_A(r - R) \right\rangle \\ &= \varepsilon_{2p} + \textit{higher order terms}. \end{aligned} \tag{5.16}$$

The same holds for the other diagonal element: $H_{BB}(\vec{r}) = \varepsilon_{2p} + \textit{higher order terms}$ . In the off-diagonal elements only the nearest neighbours at positions $R' = \pm a/2$ are considered:

$$\begin{aligned} H_{AB}(\vec{r}) &= \frac{1}{N} \sum_{R'} e^{ika/2} \left\langle \phi_A(r - R) \middle| H \middle| \phi_A(r - R - a/2) \right\rangle + e^{-ika/2} \left\langle \phi_A(r - R) \middle| H \middle| \phi_A(r - R + a/2) \right\rangle \\ &= 2t \cos\left(ka/2\right) \end{aligned} \tag{5.17}$$

where the negative quantity *t* is given by

$$t = \left\langle \phi_A(r - R) \middle| H \middle| \phi_A(r - R \pm a/2) \right\rangle \tag{5.18}$$

and $H_{BA} = H_{AB}^* = H_{AB}$ .

If we assume normalized atomic wavefunctions we get

$$S_{AA} = S_{BB} = 1$$
$$S_{AB} = S_{BA} = 2s\cos\left(ka/2\right) \tag{5.19}$$

With

$$s = \langle \phi_A(r-R) | \phi_A(r-R \pm a/2) \rangle . \tag{5.20}$$

The determinant equation giving us the energies

$$\begin{vmatrix} H_{AA} - E S_{AA} & H_{AB} - E S_{AB} \\ H_{BA} - E S_{BA} & H_{BB} - E S_{BB} \end{vmatrix} = 0 . \tag{5.21}$$

Inserting the expressions for the matrix elements leads to

$$\begin{vmatrix} \varepsilon_{2p} - E & 2(t-E)\cos(ka/2) \\ 2(t-E)\cos(ka/2) & \varepsilon_{2p} - E \end{vmatrix} = 0 . \tag{5.22}$$

The solutions for the energy are

$$E = \frac{\varepsilon_{2p} \pm 2t\cos(ka/2)}{1 \pm 2s\cos(ka/2)} \tag{5.23}$$

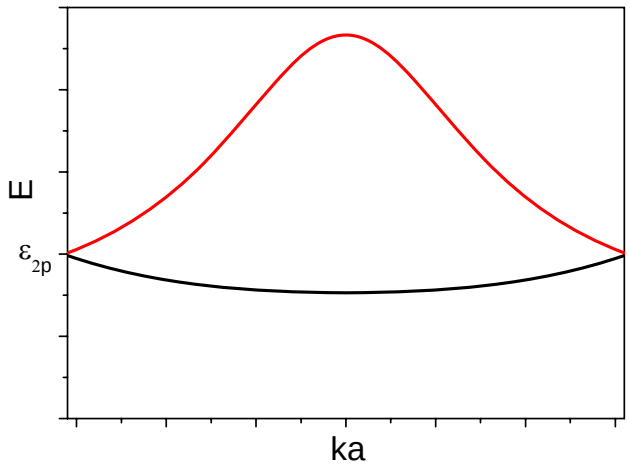


Figure 5.2 shows schematically the shape of the two bands resulting from Eq. (5.23). Each band have two states for each k-value. Each cell has 2 π-electrons (A and B). Thus both electrons are in the lower band and the energy of any electron is lower than for the *2p* electrons in free atoms. This demonstrates that the system gains energy by forming the bonds in the molecule. The lower and upper bands are often called *bonding* and *anti-bonding* states.

Fig. 5.2. Energy bands of polyacetylene.

**Exercise**: Derive the expression in Eq. (5.23)

# 6. Carbon nanostructures

A carbon nanotube can be seen as a graphene sheet rolled up into a cylinder. Before we proceed to CNT's we thus have to make a description of a two-dimensional carbon sheet.

## 6.1 Two-dimensional graphite

Figure 6.1 shows both the direct and the reciprocal lattice and unit vectors of a graphene sheet consisting of graphite atoms placed at the corners of the hexagons.

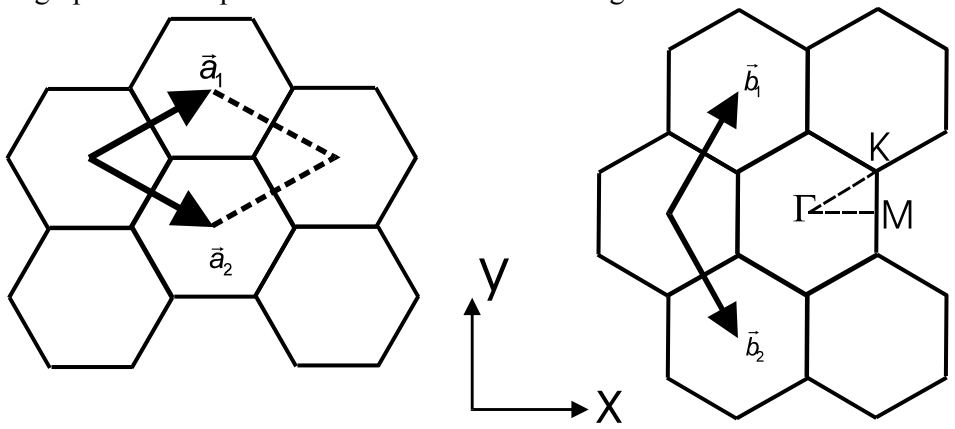


Fig. 6.1. Direct and reciprocal lattice with unit vectors for grapheme.

The lattice constant in the plane is 1.42 Å and the distance between graphite layers is 3.35 Å. It is thus possible to treat graphite as a two-dimensional system where the weak interactions among layers are neglected.
The basic vectors describing the direct and reciprocal lattice are given by (see Fig. 6.2)

$$\vec{a}_1 = a\left(\frac{\sqrt{3}}{2},\frac{1}{2}\right), \quad \vec{a}_2 = a\left(\frac{\sqrt{3}}{2},-\frac{1}{2}\right)$$

$$\vec{b}_1 = \frac{2\pi}{a}\left(\frac{1}{\sqrt{3}},1\right), \quad \vec{b}_2 = \frac{2\pi}{a}\left(\frac{1}{\sqrt{3}},-1\right) \qquad (6.1)$$

$$|\vec{a}_1| = |\vec{a}_2| = a.$$

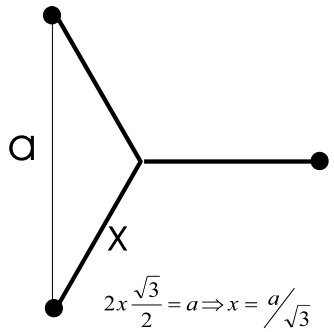


Fig. 6.2.

The lattice constant in the reciprocal lattice is $4\pi/a$ and the lattice is rotated 90° relative to the direct lattice. The 2D Brillouin zone can be translated to give the whole reciprocal lattice. From the structure we can see that each C atom has 3 nearest neighbours with which it is going to make σ-bonds in a $sp^2$ configuration. We are then left with a single π-bond in a $sp_z$-orbital in the direction perpendicular to the plane of the graphite sheet. It is these π-electrons that are responsible for the electronic and optical properties of graphite.
Let us then focus on the π-electrons. We will consider two atoms A and B and only look at nearest neighbour interaction. In this case

$H_{AA}$=$H_{BB}$ as for polyacethylene. Following the line of calculations for polyacethylene 3 neighbours at the positions $\vec{R}_1, \vec{R}_2, \vec{R}_3$ will contribute to $H_{AB}$:

$$H_{AB} = t\left(e^{i\vec{k}\cdot\vec{R}_1} + e^{i\vec{k}\cdot\vec{R}_2} + e^{i\vec{k}\cdot\vec{R}_3}\right) = t\, f(\vec{k})$$

$$= t\left[e^{ik_x a/\sqrt{3}} + e^{-ik_x a/2\sqrt{3}}\left(e^{ik_y a/2} + e^{-ik_y a/2}\right)\right] \qquad (6.2)$$

$$= t\left(e^{ik_x a/\sqrt{3}} + 2e^{-ik_x a/2\sqrt{3}}\cos\left(k_y a/2\right)\right).$$

By using that $S_{AA} = S_{BB} = 1$, $S_{AB} = S_{BA}^* = s\, f(\vec{k})$ we get the matrices

$$H = \begin{bmatrix} \varepsilon_{2p} & tf(\vec{k}) \\ tf^*(\vec{k}) & \varepsilon_{2p} \end{bmatrix}$$
$$S = \begin{bmatrix} 1 & sf(\vec{k}) \\ sf^*(\vec{k}) & 1 \end{bmatrix}. \qquad (6.3)$$

Setting the determinant of $\left[\vec{H} - E\vec{S}\right]$=0 gives the energy

$$E_{2D}(\vec{k}) = \frac{\varepsilon_{2p} \pm t\, w(\vec{k})}{1 \pm s\, w(\vec{k})} \qquad (6.4)$$

with

$$w(\vec{k}) = \sqrt{\left|f(\vec{k})\right|^2} = \sqrt{1 + 4\cos\left(k_x\sqrt{3}\,a/2\right)\cos\left(k_y a/2\right) + 4\cos^2\left(k_y a/2\right)}. \qquad (6.5)$$

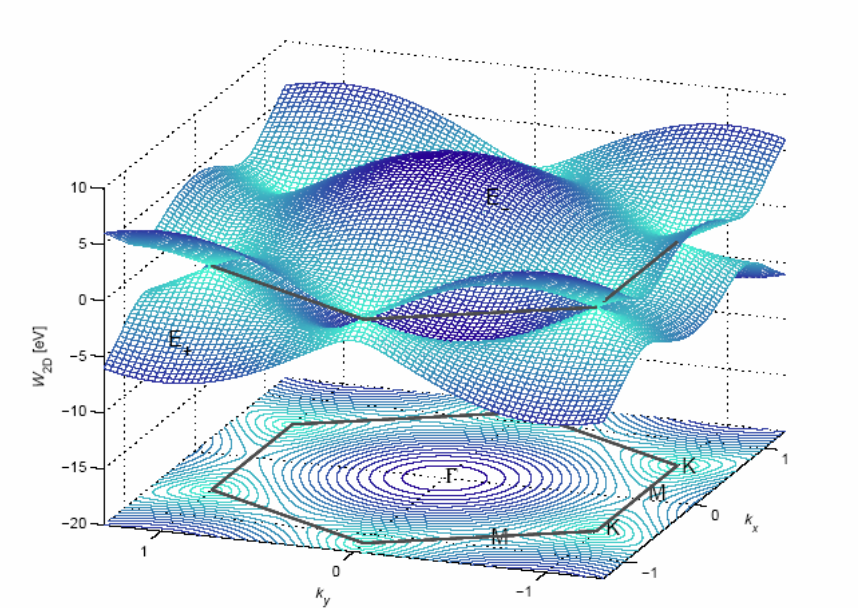


Fig. 6.3. The bonding and anti-bonding π-bands of graphene. From reference 4.

As a first approximation one can consider vanishing overlap s=0 to arrive at an energy relative to $\varepsilon_{2p}$ of the form

$$E_{2D}(k_x,k_y) = \pm t\left\{1 + 4\cos\left(\frac{\sqrt{3}\,a}{2}k_x\right)\cos\left(\frac{k_y\,a}{2}\right) + 4\cos^2\left(\frac{k_y\,a}{2}\right)\right\}^{1/2} \qquad (6.6)$$

The calculated energies from this model are shown in Fig. 6.3. With two electrons in each k-point the lower band (bonding) is full and the upper (π* antibonding) one is empty. The graphite sheet is thus a zero gap semiconductor. The width of the bands is found to be $\pm 3t$ at $k$=0.

We will not describe the σ-bands here. There will be 2 atoms per cell each contributing to 3 orbitals, in total a 6×6 matrix problem. This adds 6 bands to the two π-bands.

## 6.2 **Carbon nanotubes**

We will now consider carbon nanotubes as graphite sheets rolled up into cylinders with a limited number of carbon atoms along the circumfence. Typical diameters for single walled nanotubes are in the range from 0.7 to 2 nm while the length can be $10^4$ – $10^5$ times larger. In addition to the diameter the properties of the CNTs depend on the orientation of the C-C bonds relative to the axis of the tube. Consider the rectangle with corner at equivalent points OABB' in the graphene sheet in Fig. 6.4. The vector $\vec{T}$ is along the axis of the tube while $\vec{c}_h$ connecting points O and A is along the circumfence of the tube. The angle $\theta$ describes the direction of a cross section of the tube relative to a high symmetry direction in the sheet. Tubes with $\theta$=0 are called zig-zag tubes while those with $\theta$=30° are called armchair, in both cases refereeing to the structure of a cross section of the tube. Tubes with $\theta$ in the range $0 < |\theta| < 30^\circ$ are called chiral. A CNT is described by two integer numbers ($n$,$m$) given by $\vec{c}_h = n\vec{a}_1 + m\vec{a}_2$. It is seen directly that the CNT formed by the vectors in Fig. 6.4 is represented by (3,1).

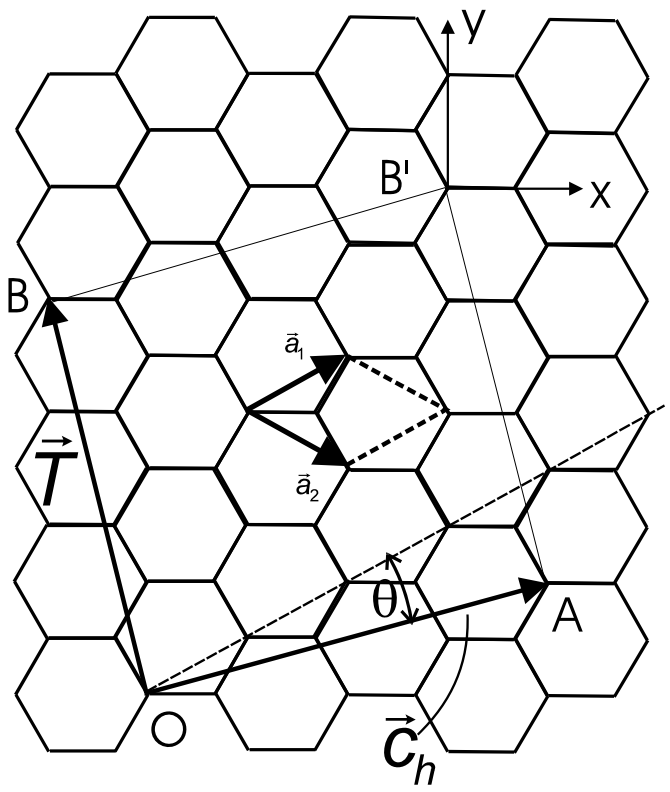


Fig. 6.4 Vectors describing the construction of a CNT from a graphene sheet.

Tubes of the type ($n$,$n$) are of the armchair type and ($n$,0) is of the zig-zag type. In terms of ($n$,$m$) the diameter of the tube is

$$d = \left|\vec{c}_h\right| / \pi = 1/\pi \, a\sqrt{n^2 + m^2 + nm}, \quad \left(\vec{a}_1 \cdot \vec{a}_2 = a^2/2\right), \tag{6.7}$$

where $a = 1.48\,\text{Å} \times \sqrt{3} = 2.49\,\text{Å}$. Also the angle $\theta$ can be expressed by ($n$,$m$):

$$\cos(\theta) = \frac{\vec{c}_h \cdot \vec{a}_1}{\left|\vec{c}_h\right|\left|\vec{a}_1\right|} = \frac{2n + m}{\sqrt{n^2 + m^2 + nm}}. \tag{6.8}$$

Furthermore, with $\vec{T}$ on the form

$$\vec{T} = t_1 \vec{a}_1 + t_2 \vec{a}_2 \tag{6.9}$$

where $t_1$ and $t_2$ are integers the orthogonality with $\vec{c}_h$ leads to

$$\vec{c}_h \cdot \vec{T} = 0 \Rightarrow a^2\left(t_1 n + \tfrac{1}{2} t_1 m + \tfrac{1}{2} t_2 n + t_2 m\right) = 0\,. \tag{6.10}$$

This is satisfied by

$$t_1 = \frac{2m+n}{d_R}, \quad t_2 = -\frac{2n+m}{d_R} \tag{6.11}$$

where $d_R$ is the largest common divisor for $(2m+n)$ and $(2n+m)$. Taking the example on Fig. 6.4 with $(n,m)=(3,1)$ we have $2m+n=5$ and $2n+m=7$ we have $d_R=1$ and thus $t_1=5$ and $t_2=-7$. The unit cell in the nanotube is OABB'. In graphene the area of the unit cell is given by $\vec{a}_1 \times \vec{a}_2$. The number of graphene unit cells $N$ in one CNT unit cell is thus

$$N = \frac{\left|\vec{c}_h \times \vec{T}\right|}{\left|\vec{a}_1 \times \vec{a}_2\right|} = \frac{2(m^2 + n^2 + nm)}{d_R}. \tag{6.12}$$

With 2 atom per graphene unit cell we have $2N$ $p_z$ orbitals in each CNT unit cell.

Figure 6.5 shows a CNT with the unit cells spanned by $\vec{c}_h$ and $\vec{T}$, each containing $2N$ carbon atoms. The position of the atoms is given by the position vector $\vec{R}$. In the reciprocal lattice rotated 90° relative to the direct lattice the lattice vector $\vec{K}_1$ is along the cicumfence (not really a vector, but the magnitudes of $\vec{K}_1$ make sense) and $\vec{K}_2$ is along the axis of the tube. As it is the case in bulk crystals vectors in direct and reciprocal space must satisfy the condition

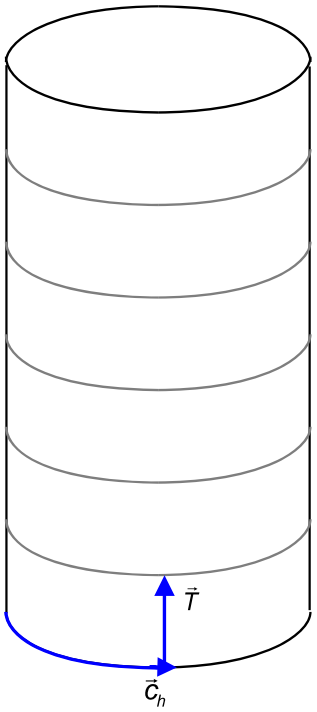

Fig. 6.5. CNT unit cell.

$$\vec{R}_i \cdot \vec{K}_j = 2\pi\delta_{ij} \tag{6.13}$$

where $\delta_{ij} = 1$ if $i=j$ and zero otherwise. Using this we get the equations

$$\begin{aligned} \vec{c}_h \cdot \vec{K}_1 &= 2\pi\,, \quad \vec{T} \cdot \vec{K}_1 = 0 \\ \vec{c}_h \cdot \vec{K}_2 &= 0\,, \quad \vec{T} \cdot \vec{K}_2 = 2\pi \end{aligned} \tag{6.14}$$

which with the forms $\vec{c}_h = n\vec{a}_1 + m\vec{a}_2$ and $\vec{T} = t_1\,\vec{a}_1 + t_2\,\vec{a}_2$ leads to

$$\begin{aligned} \vec{K}_1 &= {}^1\!/_N\left(-t_2\vec{b}_1 + t_1\vec{b}_2\right) \\ \vec{K}_2 &= {}^1\!/_N\left(m\,\vec{b}_1 - n\,\vec{b}_2\right) \end{aligned} \tag{6.15}$$

Figure 6.6 shows an example of reciprocal lattice vectors for a (4,2) CNT with $N=28$, $\vec{c}_h = (4,2)$, and $\vec{T} = (4,-5)$. We have $N$ discrete values of the $\vec{K}_1$ vector:

$$\mu\vec{K}_1\,, \quad \mu = 0,1,2,\ \cdots N-1 \tag{6.16}$$

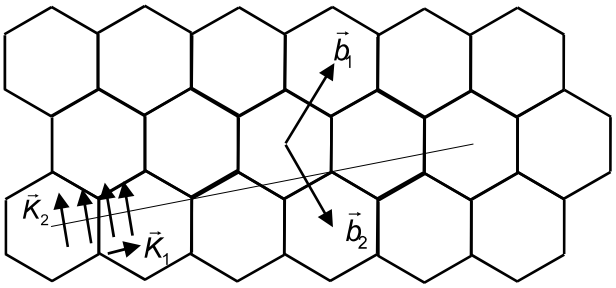


Fig. 6.6. Reciprocal lattice vectors of a (4,2) CNT.

This gives us discrete values of the wavevector in the direction along the circumfence of the CNT. Along the axis of the tube the length of $\vec{K}_2$ is $2\pi/|\vec{T}|$. If the length of the tube is $L_t$ the distance between $K_2$-values is $2\pi/L_t$. For long tubes this leads to a continuous set of $K_2$- values.

The energy bands of the CNT is obtained directly from the bands calculated for the 2D graphene sheet. Compared to the quantum wells treated earlier where discrete values of the wavevector corresponded to standing waves in the potential well the quantization in CNT's corresponds to waves that fit to the circumfence of the tube. Instead of the continuous energy surface of graphene shown in Fig. 6.3 we get a set of curves on this surface corresponding to the discrete values of $\vec{K}_2$.

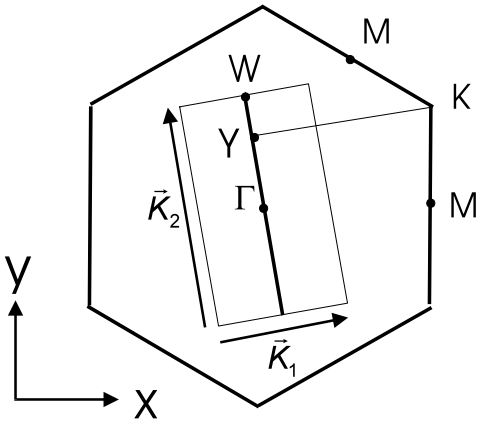


Fig. 6.7. Symmetry points in the reciprocal Brillouin zone.

Let us take the approximation in Eq. (6.6) as the two energy surfaces of the graphene sheet. The discrete energy curves of the CNT are then given by

$$E_\mu(\vec{K}) = E_{g2D}\left( k\frac{\vec{K}_2}{|\vec{K}_2|} + \mu\vec{K}_1 \right), \qquad (6.17)$$
$$\mu = 0,1,\cdots N-1,\ -\frac{\pi}{T} < k < \frac{\pi}{T}.$$

This determines the $N$ discrete energy curves. At the K-point (Fig. 6.7) the $\pi$ and the $\pi^*$ bands are degenerate (they touch). If the discrete lines passes through the K-point the CNT will be a metal. Otherwise it will be a semiconductor. The condition for this is that

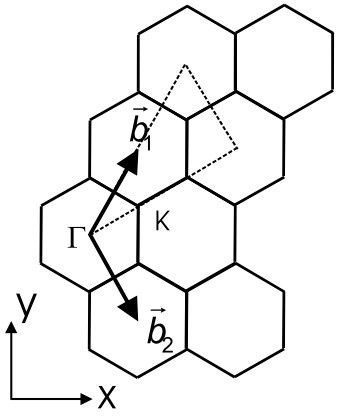


Fig. 6.8.

$\frac{\overline{YK}}{|\vec{K}_1|}$ = integer. From Fig. 6.8 it is seen that $\vec{\Gamma K} = \frac{1}{3}(2\vec{b}_1 + \vec{b}_2)$. Since

$$\vec{\Gamma K}\cdot\vec{c}_h = 2\pi\, j$$
$$\Rightarrow \frac{1}{3}\left(2\vec{b}_1 + \vec{b}_2\right)\cdot\left(n\vec{a}_1 + m\vec{a}_2\right) = 2\pi\, j \qquad (6.18)$$
$$\Rightarrow \frac{1}{3}(2n+m) = j$$

where $j$ is an integer we get the condition that CNT's with $\frac{2n+m}{3}$ equal to an integer are metals while the rest are semiconductors. This means that all armchair tubes are metals as well as the zig-zag tubes (0,0), (3,0), (6,0), · · ·. About 1/3rd of the CNT's are metallic as shown in Fig. 6.8.

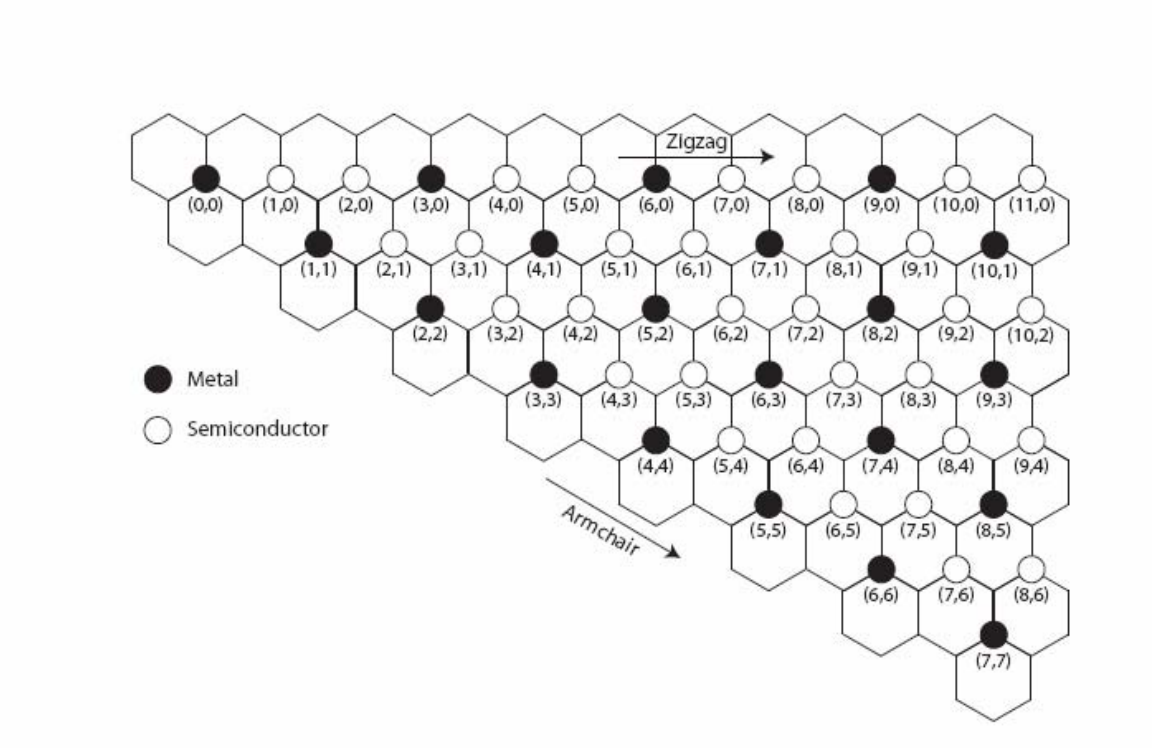


Fig. 6.8. Representation of metallic and semiconducting CNT's. From reference 4.

Consider the high-symmetry armchair structure (n,n) with the diameter $d = a\sqrt{n^2 + m^2 + nm} = a\sqrt{3}n$. Fitting a wave to the circumfence of the tube requires that $k_{x,q}d = q2\pi, \quad q = 1,2,\cdots,2n$ or

$n k_{x,q}\sqrt{3}a = 2\pi q$.

Inserting this in Eq. (6.6) gives

$$E_q(k_y) = \pm t\left\{1 + 4\cos\left(\frac{\pi q}{n}\right)\cos\left(\frac{k_y a}{2}\right) + 4\cos^2\left(\frac{k_y a}{2}\right)\right\}^{1/2}. \qquad (6.19)$$

Let $k_y$ be along the $\Gamma K$ - direction. At the zone boundary $k_y = \pi/a$ which leads us to $E_q = \pm t$. We thus have a band gap at the zone boundary. Figures 6.9 and 6.10 show the energy bands for two different CNT's. The (4,2) tube in Fig. 6.9 is semiconducting since no bands are crossing. The (3,3) tube shown in Fig. 6.10 on the other hand has bands crossing the Fermi level and are thus metallic.

**Exercise:** Derive the expressions for the reciprocal lattice vectors in Eq. (6.15).

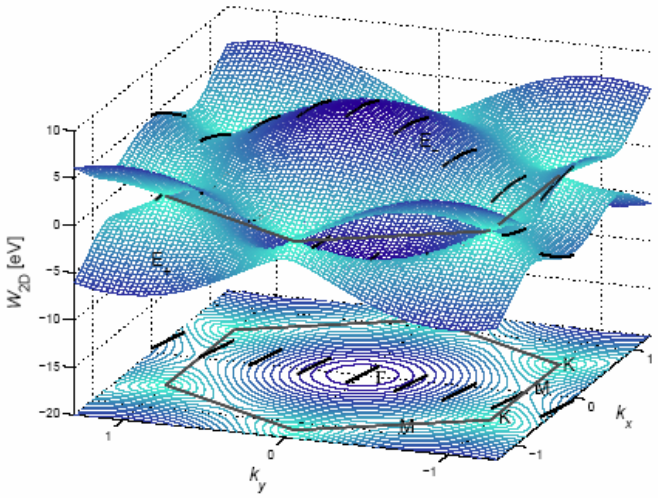


(a) Three-dimensional plot of the dispersion relation of graphene with the allowed lines plotted on the dispersion surfaces and on the contour beneath the surfaces. Not all lines are within the first Brillouin zone of graphene and are therefore not shown here. The number of lines is $N/2 = 28$ but here only $j = -4, -3, \ldots, 4$ are shown. $k_x$ and $k_y$ are in units of $\frac{\sqrt{3}a}{2\pi}$. [CD 2005, /matlab/bandstructure_graphene_confined.m]

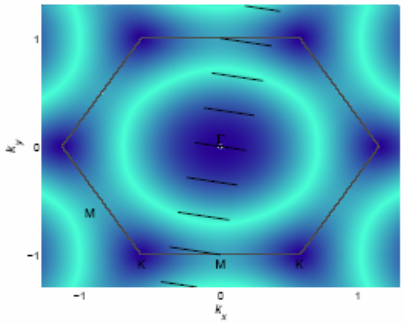


(b) A contour plot of the first Brillouin zone with allowed lines. The (4,2) nanotube is semiconducting because the allowed lines does not pass through the K-points. Not all lines are within the first Brillouin zone of graphene and are therefore not shown here. The number of lines is $N/2 = 28$ but here only $j = -4, -3, \ldots, 4$ are shown. $k_x$ and $k_y$ are in units of $\frac{\sqrt{3}a}{2\pi}$. [CD 2005, /matlab/bandstructure_graphene_confined_contour.m]

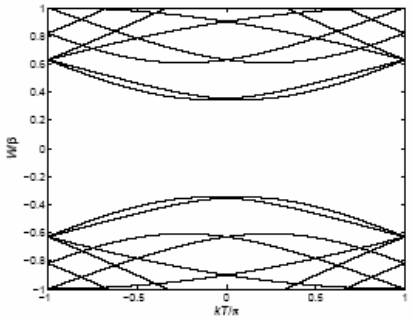


(c) The band structure obtained by means of zone folding. Only bands with energy less than $|\beta|$ are depicted here. [CD 2005, /matlab/electric_zone_folding.m]

Fig. 6.9. Energy levels of the (4,2) semiconducting CNT. From reference 4.

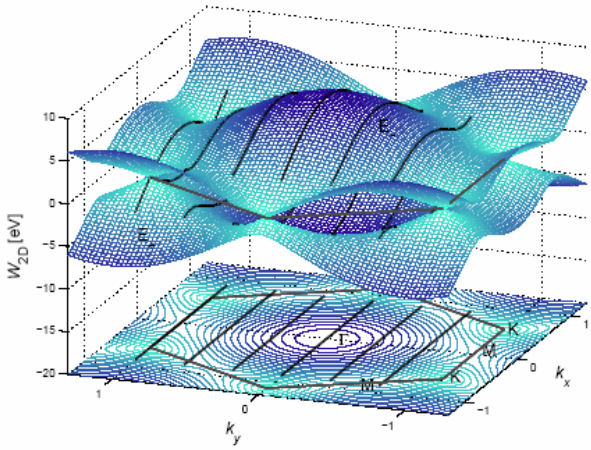


(a) Three-dimensional plot of the dispersion relation of graphene with the allowed lines plotted on the dispersion surfaces and on the contour beneath the surfaces. The number of lines is $N/2 = 6$ and $j = -3, -2, \ldots, 2$. $k_x$ and $k_y$ are in units of $\frac{\sqrt{3}a}{2\pi}$. [CD 2005, /matlab/band-structure_graphene_confined.m]

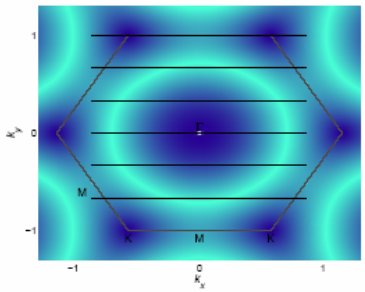


(b) A contour plot of the first Brillouin zone with allowed lines. The (3,3) nanotube is metallic because the allowed lines passes through the K-points. The number of lines is $N/2 = 6$ and $j = -3, -2, \ldots, 2$. $k_x$ and $k_y$ are in units of $\frac{\sqrt{3}a}{2\pi}$. [CD 2005, /matlab/band-structure_graphene_confined_contour.m]

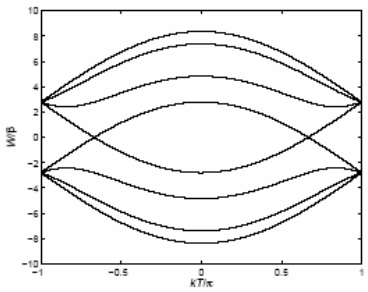


(c) The band structure obtained by means of zone folding. [CD 2005, /matlab/electric_zone_folding.m]

Fig. 6.10. Energy levels of the (3,3) metallic CNT. From reference 4.

**References:**


1. P. K. Basu, *Theory of optical processes in semiconductors*, Oxford Science Publications, 1997.
2. P. Harrison, *Quantum wells, wires and dots*, Wiley, 2005.
3. R. Saito, G&M. Dresselhaus, *Physical properties of carbon nanotubes*, Imperial College Press, 1998.
4. J. Jung, J. Bork, T. Holmgaard, N. A. Kortbek, *Single-walled carbon nanotubes*, 8th semester project, Technical Physics, 2005.